Origin of Higher Friction for Elastomers Sliding on Glassy Polymers

Betül Yurdumakan, Kumar Nanjundiah, and Ali Dhinojwala*

Department of Polymer Science, The University of Akron, Akron, Ohio 44325-3909

Received: August 10, 2006; In Final Form: October 18, 2006

We have designed a novel approach to couple infrared−visible sum frequency generation (SFG) spectroscopy with adhesion and friction measurements to determine the molecular structure of the surface molecules at the contact and sliding interfaces. The frictional force of crosslinked poly(dimethyl siloxane) (PDMS) lens sliding on poly(styrene) (PS) is a factor of 4 higher than that of PDMS sliding on poly(vinyl *n*-octadecyl carbamate-*co*-vinyl acetate) (PVNODC). This higher frictional force of PDMS/PS interface cannot be explained by its adhesion energy or hysteresis. The SFG results indicate that the hydrocarbon PVNODC surface consists of well-ordered crystalline side chains that do not restructure upon mechanical contact and during sliding of the PDMS lens. On the contrary, the SFG results show that the PS phenyl groups are more tilted upon mechanical contact and during sliding compared to that at the PS surface before contact. The change in phenyl orientation can be due to local chain interpenetration that occurs at temperatures much below the T_g of PS at the PDMS/PS interface and is the reason behind higher friction forces for PDMS elastomer sliding on glassy PS compared to that on crystalline PVNODC.

1. Introduction

It has been known for centuries that friction is related to adhesion; however, the exact relationship between adhesion and friction is still not understood.[1−4] The understanding of friction is important in areas such as energy conservation, controlling road traction of tires, nanotribology, and the design of prosthetic devices. It is intuitive that the higher the adhesion energy between two surfaces, the higher the frictional forces.[5] However, in some cases adhesion has a dissipative component (adhesion hysteresis) that has a significant influence on friction.[6,7] Early experiments by Levine and Zisman[8] as well as Briscoe and Evans[9] have shown that the friction for fluorocarbon surfaces was higher than that for hydrocarbon surfaces even though the fluorocarbon surfaces have lower adhesion energy. Chaudhury and Owen[6] suggested that the cause of higher friction for poly(dimethyl siloxane) (PDMS) lenses sliding on fluorocarbon surfaces was related to adhesion hysteresis. The higher friction for fluorocarbon surfaces was attributed to partial interdigitation of the chains across the interface increasing the dissipation of energy during sliding.

The interdigitation of molecules at the interface was suggested as a cause of higher adhesion hysteresis and higher friction for many different systems. Israelachvili and co-workers[7] have shown that the amorphous state of the self-assembled monolayers (SAM) show highest friction in comparison to crystalline and liquidlike monolayers. The amorphous layers interdigitate and this leads to high friction in comparison to the crystalline monolayers. The liquidlike monolayers interdigitate but have lower viscosity, and this results in lower friction. To correlate friction and adhesion hysteresis, Israelachivili and co-workers proposed that the frictional stress was equal to $\Delta W/\delta$ where ΔW was the adhesion hysteresis and δ was the length of the interdigitation. Both ΔW and δ depend on the level of interdigitation.[7] Similar enhancement in friction because of interpenetration were observed in polymer−polymer sliding.[10,11] Brown[10] showed that the higher friction of PDMS lenses sliding on surfaces with tethered (or grafted) polymer chains can be explained by the interpenetration of tethered chains into the crosslinked rubber. Israelachvili and co-workers[11] reported a factor of 10 increase in friction for UV exposed polystyrene (PS) surfaces in comparison to sliding on crosslinked PS surfaces. The UV exposure results in chain scission and the creation of free chain ends that can penetrate and increase the friction similar to the case observed by Brown using tethered chains on surfaces.

Although there is mounting evidence for a strong correlation between adhesion, adhesion hysteresis, and friction, there still are some striking anomalies. Vorvolakos and Chaudhury reported much higher shear stress for PDMS elastomer sliding on PS surfaces in comparison to a well-packed hydrocarbon monolayer (SAM).[12] This was unexpected because the adhesion energies of the PDMS/SAM and PDMS/PS interfaces are only slightly different. In addition, the adhesion behavior of both interfaces were found to be nonhysteretic. This behavior contradicts with the observations of fluorocarbon surfaces in which the higher friction was explained by the increase in adhesion hysteresis.[6] Roughness was also ruled out because the two surfaces were smooth down to the nanometer level (0.2 nm for the monolayer and 0.5 nm for PS). Vorvolakos and Chaudhury have pointed that the higher shear stress for PDMS/PS could be due to interdigitation of PS chains in the PDMS elastomer. If we consider that an adhesion hysteresis of 1 mJ/m^2 cannot be resolved experimentally and assume a local penetration of ≈0.5 nm (the size of a phenyl group), we obtain an upper limit of 2 MPa variation in the friction force. This could explain the difference in the shear stress between PDMS/SAM and PDMS/PS interfaces. However, it is not clear why we should expect interpenetration across the interface between a glassy polymer and a crosslinked rubber. Brown has also shown that the friction forces of PDMS sliding on a glassy PS surface are much higher than that on a PDMS surface.[10] Brown interpreted his finding as the rigid PS slowing down the

* Corresponding author. E-mail: ali4@uakron.edu.

10.1021/jp0651687 CCC: $37.00
Published on Web 12/10/2006

molecular mobility of the PDMS segments at the interface leading to higher energy dissipation during sliding. Both these arguments, mobility and interpenetration, involve the changes in the structure of the interfacial molecules upon contact or during sliding.

The studies mentioned above reveal the complexity of friction, adhesion and their relationships. Thus, the need for a technique that can probe the structure of the interfacial molecules is vital. For this purpose, we designed an approach to couple the infrared−visible sum frequency generation (SFG) spectroscopy to study molecular structure (orientation and density of molecules) at the polymer/solid and polymer/polymer interfaces[13,14] with adhesion and friction experiments. We have already demonstrated that SFG in total internal reflection (TIR) geometry can be used to directly probe the molecular structure at the elastomer/polymer contact interfaces.[14,15] We have taken advantage of a well-characterized model elastomeric network, PDMS, to generate large uniform contact area with the polymer surfaces. The size of the contact area can be controlled by the applied load and radius of curvature of the lens based on the Johnson, Kendall, and Roberts (JKR) theory.[16] We have investigated the interface of PDMS/PS and PDMS/poly(vinyl *n*-octadecyl carbamate-*co*-vinyl acetate) (PVNODC). These systems are similar to that studied by Vorvolakos and Chaudhury.[12] We have used PVNODC instead of the SAM because it is easier to prepare smooth surfaces. We have shown before that the surface of PVNODC is similar to that of SAM.[17] The octadecyl side chains crystallize predominantly in all-trans conformation with the side chains aligned perpendicular to the surface. The surface energies of PVNODC and SAM as well as the adhesion energies of PDMS/PVNODC and PDMS/SAM interfaces are similar.

2. Experimental Section

2.1. SFG Measurements. SFG is a second-order nonlinear optical technique that is sensitive to the orientation and concentration of molecules at interfaces. The details of the SFG theory and the SFG spectrometers have been discussed previously.[18,19] Briefly, SFG involves mixing a visible high-intensity laser beam of frequency ω_{vis} with a tunable infrared wavelength source of frequency ω_{ir}. According to the dipole approximation, generation of SFG photons (at frequency $\omega_{vis} + \omega_{ir}$) is forbidden in the centrosymmetric bulk but allowed at the interface in which the inversion symmetry is broken. The SFG intensity is resonantly enhanced when ω_{ir} overlaps with the resonant frequency of the vibration modes of the surface molecules. The value of the resonance frequency provides the identification of the chemical groups present at the interface. In addition, the intensities of the asymmetric and symmetric vibrations in the SFG spectra provide information on the orientation of these chemical groups at the interface.[13,15,20,21] The TIR geometry further enhances the SFG intensity by 1−2 orders of magnitude.[13] By the proper choice of incident angles in TIR, we have selectively probed the contact interface while reducing the contribution from the other interfaces. We have used 42° for the polymer surfaces, while 8° or 12° were chosen for the elastomer/polymer interfaces.

2.2. Adhesion Measurements. For adhesion measurements, a home built apparatus similar to the one described by Qi et al. was used.[22] On the basis of a protocol developed by JKR,[16] the contact area between a compliant hemispherical PDMS lens and a flat substrate is measured as a function of force during loading (approaching two surfaces) and unloading (separating two surfaces).[23] This allows the estimation of the work of adhesion, W_a, by

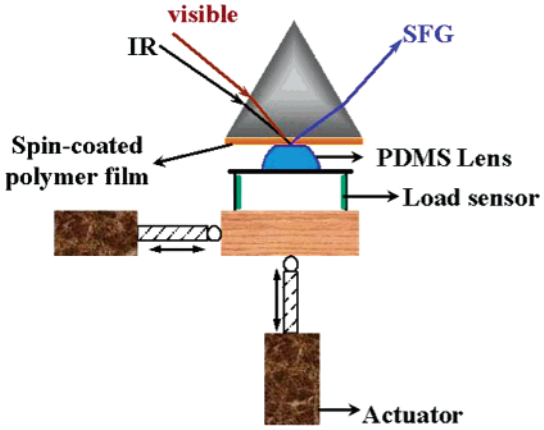

Figure 1. Schematic diagram of the friction apparatus for in situ adhesion and friction measurements using SFG in TIR geometry.

$$a^3 = \frac{R}{K}[P + 3\pi RW_a + \sqrt{6\pi RW_aP + (3\pi RW_a)^2}] \quad (1)$$

where a is the radius of contact, R is the radius of curvature of the hemisphere, P is the applied load, and K is the elastic constant of the system. The adhesion measurements in this study were performed by increasing or decreasing the load in steps of ≈200 μN at 5 min intervals. The apparatus was kept on a vibration damping table and the humidity and temperature were 35−45% and 20−24 °C, respectively.

The JKR theory is based on an equilibrium state in which the elastic forces are balanced by the interfacial forces. In this case, the mechanically applied energy that is available to decrease the contact area by a unit amount is equal to the thermodynamic work of adhesion. This energy is often called the energy release rate or fracture energy, G, expressed by

$$G = \frac{\left(P - \frac{a^3K}{R}\right)^2}{6\pi Ka^3} \quad (2)$$

When $G = W_a$, the separation of the two surfaces does not involve energy dissipation. The work necessary for this process is a direct measure of W_a as stated in the JKR theory. However, considerable amount of energy may be dissipated irreversibly during the formation of new surfaces. Therefore, G may be higher than W_a indicating that more energy is needed to separate the two surfaces than to form an interface by bringing them together. This phenomenon is known as adhesion hysteresis and indicates that nonequilibrium processes take place at the interface such as interdigitation, restructuring, disentanglement, and inelastic deformations.[6]

2.3. Friction Measurements. The friction measurements were conducted using a home built apparatus based on the design described by Barquins (Figure 1).[24] A PDMS lens attached to a thick aluminum (Al) plate with a double-sided stick tape was pressed against the sample surface. Then, an increasing tangential force was imposed on the Al plate. The contact area was measured before and during sliding. A rigid Al plate was used to keep the distance between the plate and sample surface constant to reduce the changes in the contact area during sliding. The normal load was estimated by comparing the contact area during friction with the contact area during

the JKR measurements using similar conditions. The friction force was measured using strain gauges (sensitivity of ≈3960 μV/g ± 3%) attached to the spring steel pillars holding the Al plate. The spring constant was determined by measuring displacement as a function of weight ($k \approx 300$ mN/m). The force was recorded in voltage as a function of time. For most measurements, a slight (≈1%) reduction in contact area occurred during sliding. The tangential force was divided by the contact area to obtain the shear stress that was plotted as a function of time. When the interfaces exhibited stick−slip dynamics, similar to that reported by Grosch,[25] the values at the highest point (stick) were averaged. The friction measurements were performed for each lens/surface pair at various normal loads and sliding velocities. The values of shear stress were independent of the normal load and the contact area, which is consistent with previous findings of Homola and co-workers[26] as well as Chaudhury and co-workers.[6,27] This indicates that the actual and apparent contact areas change with load in a similar manner. The values of shear stress were independent of velocity in the range from 0.5 to 15 μm/s.

2.4. Sample Preparations. The crosslinked PDMS lenses were prepared by mixing a desired amount of divinyl-terminated PDMS (6000 g/mol) with 10% crosslinker, poly(methylhydrosiloxane−dimethylsiloxane) copolymer (1950 g/mol). A platinum−cyclovinylmethyl complex (3−3.5% Pt) was added as a catalyst (10 μL for each gram of mixture). All materials were purchased from Gelest, Inc., and used as received. The PDMS mixture was stirred thoroughly for at least 1 min. Any air bubbles that were generated during mixing were removed by letting the mixture stand for several hours before preparing the lenses for JKR and SFG measurements. The lenses for the JKR measurements were prepared by placing small drops of the mixture on fluorosilane treated glass slides using a syringe needle and then curing at 60 °C for 4 h. The lenses for the friction measurements, which are bigger in size compared to those for JKR measurements, were prepared by placing drops of the same mixture on the surface of a sterilized PS petri dish filled with distilled water. These lenses were first cured at room temperature overnight and then further cured at 60 °C for 4 h in the presence of water. After the curing was completed, the water was poured out, the lenses were gently dried under a slight flow of N_2, and then were dried completely at 60 °C overnight under vacuum. The sol fraction (unreacted precursor) of the lenses were extracted with toluene. The lenses were placed in a beaker lined with a filter paper and swelled in excess amount of toluene for 2 days. Then, the solvent was changed every day for 4−5 days. At the end, the solvent was removed, and the sheets and lenses were first dried overnight in air at room temperature and then were further dried overnight under vacuum at 60 °C.

These lenses were pressed against the flat surface of glass or sapphire substrates or the flat surface of sapphire prisms that was spin coated with a 2−4 wt % solution of PVNODC or PS in toluene at 2000 rpm. The polymer films were annealed in vacuum for 3−4 h at 110 °C. The thickness of the PS and PVNODC films were 300 nm (measured using ellipsometry). PVNODC ($M_w = 70$ kg/mol, polydispersity index (PDI) = 3.0) was a gift from 3M Corporation and PS ($M_w = 108$ kg/mol, PDI = 1.06) was purchased from Polymer Sources. Both polymers were used as received.

The root-mean-square roughness of the PDMS elastomer and polymer films were measured with an atomic force microscopy (AFM) (Digital Instruments Nanoscope IIIa multimode). AFM measurements were performed with tapping mode at 0.5 Hz scan rate to prevent deformations or irreversible displacements.

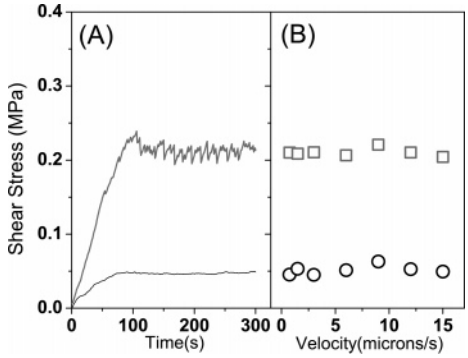

Figure 2. (A) Shear stress as a function of time for PDMS sliding on PVNODC (black line) and PS (gray line) at a velocity of 3 μm/s. (B) The shear stress during sliding plotted as a function of velocity for PDMS sliding on PVNODC (○) and on PS (□).

Standard rectangular silicon cantilevers (MikroMasch) with a typical radius of curvature <10 nm and a spring constant of ≈3.5 N/m (supplied by the manufacturer) were used. Roughness values were found to be less than 0.5 nm for PDMS elastomer, 0.2 nm for PVNODC, and 0.5 nm for PS.

3. Results and Discussion

3.1. Friction Results. Figure 2 shows the friction data for PDMS lenses sliding on PVNODC and PS surfaces. After the initial static force, a smooth and stable sliding is observed for PDMS/PVNODC, while the sliding has an irregular sawtooth profile for PDMS/PS systems. This sawtooth modulation is characteristic of stick−slip sliding in which the sliding surfaces alternately switch between sticking and slipping. The stick−slip behavior is related to energy loss during sliding.[28] It occurs below a critical velocity that is the transition point to smooth sliding. Because of the velocity limit of the friction apparatus used in this study, we have observed stick−slip sliding for PDMS on PS at all velocities. In the case of stick−slip sliding, the maximum force just before slip is recorded to determine the shear stress.[25] Shear stress as a function of velocity is plotted in Figure 2B. As expected for low velocity, the values of shear stress do not depend on the velocity and are load independent. The shear stress of PDMS sliding on PS is about 4 times higher than that of PDMS sliding on PVNODC. This ratio is consistent with that reported by Vorvolakos and Chaudhury.[12,29]

3.2. Adhesion Results. To correlate the friction behavior with adhesion, JKR experiments were performed between PDMS/PVNODC (Figure 3A,B) and PDMS/PS (Figure 3C,D) interfaces. Figure 3A,C show the contact radius cubed, a^3, as a function of the applied load and Figure 3B,D show strain energy release rate, G, as a function of a. The G from the loading data are 48 mJ/m^2 for PDMS/PVNODC and 55−56 mJ/m^2 for PDMS/PS. In addition, both interfaces have negligible adhesion hysteresis, and thus we can assume that $G = W_a$. A theoretical value of W_a can be calculated assuming only dispersion forces ($W_a = 2(\gamma_1\gamma_2)^{0.5}$). The critical surface energies of PDMS, PVNODC, and PS are calculated from contact angles of various liquids by geometric mean equation. The liquids used are distilled water, diiodomethane, and ethylene glycol.

The average of the calculated values from each pair of liquids gives the surface energies of PDMS, PVNODC, and PS as 21.7, 23.1, and 41.4 mJ/m^2, respectively. These values are consistent with those reported in the literature.[30] Assuming only dispersion forces, we predict $W_a \approx 45$ mJ/m^2 for the PDMS/PVNODC, and $W_a \approx 60$ mJ/m^2 for the PDMS/PS interfaces. The experimental W_a values are in good agreement with the theoretical

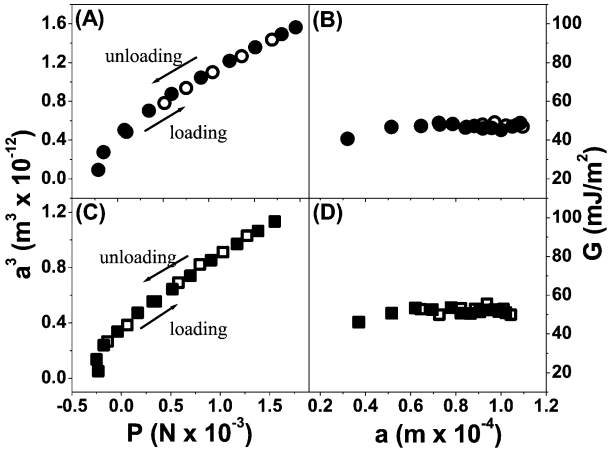

Figure 3. JKR plots of PDMS on PVNODC (○) and PS (□) during loading (open symbols) and unloading (filled symbols). (A) and (C) shows the contact radius cubed, a^3, as a function of the applied load. In (B) and (D), the strain energy release rate is plotted as a function of the contact radius.

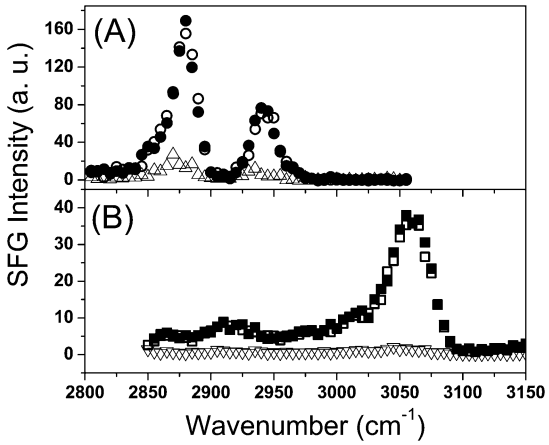

Figure 4. (A) SFG spectra in SSP polarization for PVNODC before contact (filled ○), during contact (△), and after the PVNODC surface has experienced sliding (○). (B) SFG spectra in SSP polarization for PS before contact (filled □), in contact (▽), and after the PS surface has experienced sliding (□).

predictions. The ratio of the adhesion energies measured for PDMS/PS and PDMS/PVNODC is ≈1.3, much smaller than the ratio of the shear stress if we assume that the shear stress is directly proportional to the adhesion energy. Because the adhesion hysteresis is negligible at both interfaces, we can conclude that neither adhesion nor adhesion hysteresis provide an explanation for the large difference in shear stress.

3.3. SFG Results. Figure 4 shows the SFG spectra for PVNODC and PS surfaces in the SSP polarization (S-polarized SFG beam, S-polarized visible beam, P-polarized IR beam) at an incident angle of 42°. At this incident angle, the SFG spectra correspond to the PVNODC or PS/air surfaces. The interfacial area during contact and sliding is kept larger than the laser spot in these experiments to avoid any SFG signal contribution from outside the contact area. The filled symbols in Figure 4 correspond to the SFG spectra of the PVNODC (Figure 4A) and PS (Figure 4B) surfaces before bringing them in contact with the PDMS lens. The SFG spectra shown in Figure 4 as open triangles are measured during contact. Here, the SFG signals are much weaker because the incident angle of 42° is far from the critical angle for the PDMS/polymer interface. The SFG spectra shown as open circles (PVNODC) and open squares (PS) in Figure 4 are acquired after the PDMS lens has slit across

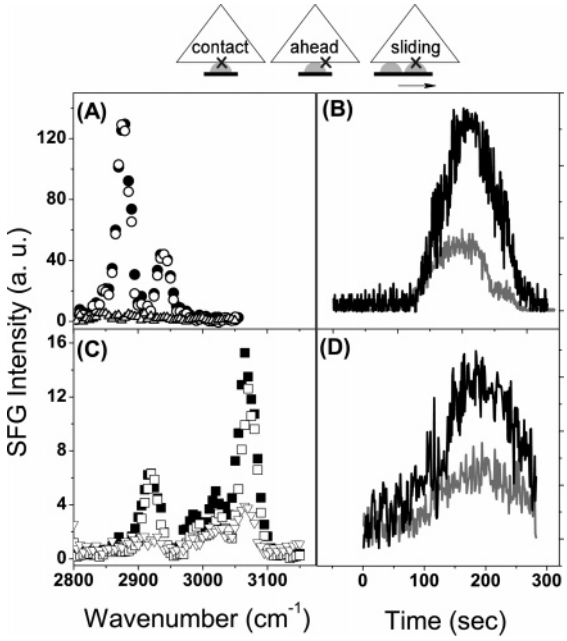

Figure 5. The sketch illustrates the experimental geometry used to probe the SFG spectra during contact and sliding. (A) and (C) show the SFG spectra in the SSP polarization for PDMS/PVNODC (○) and PDMS/PS (□) acquired during contact (filled symbols) when the laser beam is ahead of the contact spot (Δ, ▽), and after sliding the lens to superimpose the contact spot and the laser beam again (open symbols). (B) The plot of the SFG intensity as a function of time associated with the r^+ (black line) and r_{Fr}^+ (gray line) of the methyl groups of the PVNODC side chains. (D) The plot of the SFG intensity as a function of time associated with the phenyl vibrations (υ_2, black line) of the PS side chains, and 2906 cm^{-1} (gray line) associated with the symmetric vibration of PDMS methyl groups. In (B) and (D), we start with the laser spot ahead of the contact area, and the SFG intensities are low in the beginning. When the contact area overlaps with the laser beam, we observe the maximum SFG intensity. After the contact area passes the laser spot, once again the SFG intensity drops.

the contact spot. The peaks in the PVNODC spectrum in Figure 4A are assigned to the methyl symmetric vibration (r^+) at ≈2875 cm^{-1} and Fermi resonance (r_{Fr}^+) at ≈2935 cm^{-1}. This spectrum is similar to the SSP spectrum of SAM reported previously[15] and indicates a surface structure expected for well-packed alkyl side-chains of PVNODC in predominantly all-trans conformation. The peaks in the PS spectrum in Figure 4B corresponds to the phenyl C−H stretching modes of PS. The dominant peak at ≈3065 cm^{-1} is assigned to the υ_2 symmetric vibration. There is a small contribution from the vibration of the methylene groups (2920 cm^{-1}). This spectrum is similar to that observed previously at the PS surface where the average orientation of the phenyl rings is parallel to the surface normal.[13] The most important outcome from Figure 4 is that the spectra after sliding, for both PVNODC and PS surfaces, are identical to those before contact. This indicates that either the surface molecules are not affected from sliding or the molecular changes that took place during sliding are reversible.

The structure during contact is directly probed in situ using the incident angle of 8° for the PDMS/PVNODC and 12° for the PDMS/PS interfaces. It will be helpful to understand the experimental procedure before discussing the SFG results. The sketch of the experimental geometry is shown in Figure 5. The symbol "X" corresponds to the spot that is probed using the laser beams. The filled symbols in Figure 5A,C correspond to the situation where the laser beam is superimposed with the contact spot (area) at the interface. The open triangles in Figure 5A,C correspond to the situation where the laser beam is

positioned in front of the contact area. In this condition, the incident angle is far away from the critical angle for the PDMS/polymer interface, and the SFG intensity is much weaker than that observed when the laser beam and the contact spot are superimposed. Any spectral features observed at this state are a combination of signals from the polymer/sapphire interface and polymer surface. The open circles (PDMS/PVNODC) and open squares (PDMS/PS) correspond to the situation in which the laser beam was positioned in front of the contact spot at the beginning, and then the lens was moved with the desired speed. The SFG spectra were acquired after the lens once again overlapped with the laser spot. In this condition, we are probing the contact interface that has experienced sliding.

First, we will discuss the SFG spectra of the PDMS/PVNODC (Figure 5A) and PDMS/PS (Figure 5C) contact interfaces. The peak assignments of the PDMS/PVNODC interface are similar to those of the PVNODC surface. The two main peaks correspond to the vibrations of the terminal CH_3 groups of the PVNODC side chains. The contributions from the $Si-(CH_3)_2$ groups of the PDMS segments are expected at $\approx$2906 cm^{-1} (symmetric, r^+_{PDMS}) and at $\approx$2962 cm^{-1} (asymmetric, r^-_{PDMS}). At this interface, the intensities of the PDMS peaks are negligible in comparison to the peak intensities of the well-ordered PVNODC side chains. The structure of the contact interface is very similar to the PVNODC surface, which is expected for a crystalline structure. In the case of PDMS/PS interface, the two main peaks below 3000 cm^{-1} correspond to the r^+_{PDMS} and r^-_{PDMS} vibrations of the $Si-(CH_3)_2$ groups of PDMS. Above 3000 cm^{-1}, the dominant contribution is from the υ_2 symmetric vibration (3060 cm^{-1}) with a shoulder at 3025 cm^{-1}, which is slightly higher than that observed at the PS surface. The SFG spectrum of the area ahead of the contact are shown as open triangles in Figure 5A,C. Because there is no contact interface here, these spectral features are characteristics of both the PS/sapphire interface and PS surface generated at an off critical angle.[13,21]

It was not possible to acquire a complete spectrum during sliding, because the time to acquire a spectrum takes 10−15 min. Instead, we have monitored the intensity of selected vibrations from the interface as a function of time (Figure 5B,D). We first position the laser spot ahead of the contact area and then begin sliding the lens toward the laser spot. Initially, the SFG intensity is weak because it is collected from the area ahead of the contact interface. Then, the SFG intensity increases and reaches a plateau when the lens starts to overlap with the laser beam. After the lens slides past the laser spot, the SFG intensity drops back to its original low value. Figure 5B shows the $I^{PVNODC}_{r^+}$ and $I^{PVNODC}_{r^+_{FR}}$ as a function of time. The ratio of the average intensities at the plateau, $I^{PVNODC}_{r^+_{FR}} / I^{PVNODC}_{r^+}$, is $\approx$0.34 during sliding. The ratio of $I^{PVNODC}_{r^+_{FR}} / I^{PVNODC}_{r^+}$ $\approx$ 0.33 and 0.32 for the PDMS/PVNODC interface before and after sliding, respectively. The similarity between these three numbers indicates that there is very small difference, if any, in the spectral features of the PDMS/PVNODC interface before, after, and during sliding. Consequently, we can argue that neither adhesion nor friction affects the molecular structure of PVNODC side chains as expected for a crystalline surface. In the case of PDMS/PS interface (Figure 5C), we obtain the ratio of $I^{PDMS}_{r^+}/I^{PS}_{\upsilon_2}$ $\approx$ 0.38 and 0.43 before and after sliding, respectively. The analysis of contact interface during sliding from Figure 5D indicates that the peak ratio ($\approx$0.36) is similar to the one at the contact before sliding. Thus, the spectral features of the PDMS/PS interface do not show observable changes during sliding.

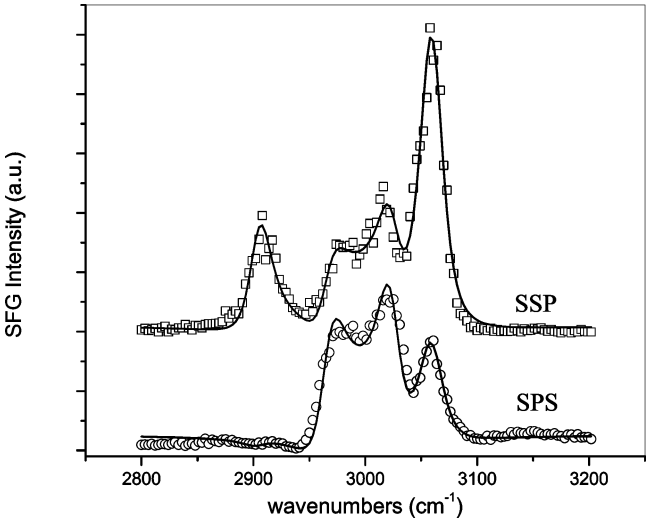

Figure 6. SFG spectra for the PDMS/PS interface in SSP (□) and SPS (○). The SSP spectrum is shifted vertically for improving the clarity. The solid lines are fit to a Lorentzian equation discussed in the text.

So far, neither adhesion behavior nor the spectral features in the SFG measurements during sliding explain the difference between the values of shear stress encountered in sliding PDMS on PVNODC and PS. However, we believe that the structural changes have already taken place upon mechanical contact at the PDMS/PS interface. To analyze the changes in the orientation of the phenyl groups at the PDMS/PS interface, we have compared the SFG spectra in SSP and SPS polarization in Figure 6. The SPS spectrum shows three peaks associated with the asymmetric vibration of the methyl group of PDMS (2965 cm^{-1}) and asymmetric (υ_{20b}, 3025 cm^{-1}) and symmetric (υ_2, 3060 cm^{-1}) vibrations of the phenyl groups. The ratio of the symmetric phenyl vibrations in the SPS and SSP polarization is related to the orientation of the phenyl groups at the interface. We also can calculate the relative contribution of the phenyl groups by fitting the spectra using the following Lorentzian equation (shown as solid lines in Figure 6):[13]

$$I(\mathrm{SFG}) \propto \left| \chi_{\mathrm{eff,NR}} + \sum_q \frac{A_q}{\omega_{\mathrm{IR}} - \omega_q - \mathrm{i}\Gamma_q} \right|^2 \qquad (3)$$

where A_q, Γ_q, and ω_q are the strength, damping constant, and angular frequency of a single resonant vibration, respectively. $\chi_{\mathrm{eff,NR}}$ is the nonresonant part of the signal.

To quantify the changes in the tilt angles, we have plotted the prediction of $|A_{q,\upsilon_2 \text{ or } 20b}(\mathrm{SPS})/A_{q,\upsilon_2 \text{ or } 20b}(\mathrm{SSP})|$ as a function of tilt angle in Figure 7. The details of this SFG analysis are provided in previous publications.[31] On the basis of the experimentally determined ratios of A_q, we estimate from Figure 7 that the phenyl groups are tilted with an angle of 30−40° with respect to the surface normal. This tilt angle (30−40°) of the phenyl groups at PDMS/PS interface is larger than the 20° determined at the PS/air surface.[13] We interpret the changes in the orientation of the phenyl groups as the consequence of local interpenetration at the PDMS/PS interface.

This interdigitation across the interface between a crosslinked elastomer and glassy polymer is unexpected. However, based on the arguments presented by Chaudhury, a penetration as small as 0.1−0.5 nm can result in significant enhancement of friction.[12] Thus, the penetration does not need to be at the length

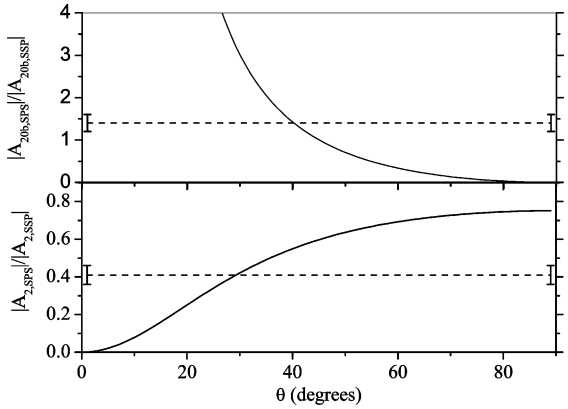

Figure 7. The prediction of $|A_{q,\nu_2 \text{ or } 20b}(\text{SPS})/A_{q,\nu_2 \text{ or } 20b}(\text{SSP})|$ as a function of tilt angle of PS phenyl groups with respect to the surface normal. The experimental values determined from the fit in Figure 6 are shown in the figure as dotted lines.

scale of R_g or even at a length scale associated with T_g. An interpenetration of the phenyl groups at a local level is sufficient to explain the high friction forces at the PDMS/PS interface. Interestingly, an activation energy corresponding to sub-T_g relaxation process also was observed for frictional forces measured using scanning force microscopy (SFM).[32] This activation energy was attributed to the hindered rotation of the phenyl groups, which are dissipating energy during sliding of the silicon tip on the PS surface. Similarly, we propose that the energy dissipation during sliding occurs because of the phenyl groups that have intermingled at the PDMS/PS contact interface, which results in higher friction. This local change in interfacial structure for PDMS in contact with PVNODC film is not possible because the surface of the PVNODC film is covered with crystalline alkyl side chains. However, a contact interface between PDMS/PVNODC would exhibit local interpenetration and higher friction if it was heated above the melting point of PVNODC. These experiments are in progress.

4. Conclusions

By using interface sensitive SFG spectroscopy, we have shown direct evidence of change in orientation of PS phenyl groups that indicates local interpenetration at the contact interface of PDMS with glassy PS. We postulate that this effect may be general for other glassy polymers. The changes in the orientation of the phenyl groups are reversible, and the structure before contact is recovered once the PDMS lens is removed from contact. This interpenetration is absent for PDMS in contact with side chain crystalline PVNODC. This explains the higher friction forces for PDMS lenses sliding on PS surfaces in comparison to those sliding on PVNODC surfaces. Several hypotheses may explain the local interpenetration. First, from equilibrium thermodynamic arguments, a finite interfacial width is expected for the contact interface between PDMS and PS segments even though these two polymers are immiscible. Second, the penetration is at such a small length scale (phenyl groups) that this effect is due to sub-T_g relaxations, and T_g of the bulk PS film is not the determining factor for these local rearrangements. Third, one could argue that the surface of the PS film is more mobile than the bulk that has been observed with several experimental techniques.[33] Last, it is possible that the mobile PDMS chains act as a local plasticizer and increase the mobility of the PS surface groups. In the past, interpenetration across an interface has been suspected to cause energy dissipation during friction, but this always was accompanied with adhesion hysteresis. A local interpenetration that is unresolved by adhesion measurements, even though it has a profound influence on the frictional forces, requires a direct experimental technique like SFG that can provide information on the structure of molecules at the static and dynamic interface.

Acknowledgment. We gratefully thank the financial support from NSF (DMR-0512156 and CTS-0355304). We also thank Professor Cheng (University of Akron) for use of his AFM instrument, Professor Brittain (University of Akron) for use of his contact angle instrument, and Edward Laughlin (University of Akron) for machining the friction cell.

References and Notes

(1) Briscoe, B. J.; Tabor, D. *Faraday Spec. Discuss. Chem. Soc.* **1972**, *2*, 7−22.

(2) Singer, I. L.; Pollock, H. M. *Fundamentals of Friction;* Kluwer Academic Publishers: Dordrecht, The Netherlands, 1992.

(3) Persson, B. N. J. *Physics of Sliding Friction;* Kluwer Academic Publishers: Dordrecht, The Netherlands, 1996.

(4) Persson, B. N. J. *Sliding Friction: Physical Principles and Applications;* Springer: Heidelberg, Germany, 1998.

(5) McFarlane, J. S.; Tabor, D. *Proc. R. Soc. London* **1950**, 244−253.

(6) Chaudhury, M. K.; Owen, M. J. *Langmuir* **1993**, *9*, 29−31.

(7) Yoshizawa, H.; Israelachvili, J. *J. Phys. Chem.* **1993**, *97*, 11300−13.

(8) Levine, O.; Zisman, W. A. *J. Phys. Chem.* **1957**, *61*, 1068−1077.

(9) Briscoe, B. J.; Evans, D. C. B. *Proc. R. Soc. London, Ser. A* **1982**, *380*, 389−407.

(10) Brown, H. R. *Science* **1994**, *263*, 1411−1413.

(11) Maeda, N.; Chen, N.; Tirrell, M.; Israelachvili, J. N. *Science* **2002**, *297*, 379−382.

(12) Vorvolakos, K.; Chaudhury, M. K. *Langmuir* **2003**, *19*, 6778−6787.

(13) Gautam, K. S.; Schwab, A. D.; Dhinojwala, A.; Zhang, D.; Dougal, S. M.; Yeganeh, M. S. *Phys. Rev. Lett.* **2000**, *85*, 3854−3857.

(14) Harp, G. P.; Dhinojwala, A. *J. Adhes.* **2005**, *81*, 371−379.

(15) Yurdumakan, B.; Harp, G. P.; Tsige, M.; Dhinojwala, A. *Langmuir* **2005**, *21*, 10316−10319.

(16) Johnson, K. L.; Kendall, K.; Roberts, A. D. *Proc. R. Soc. London, Ser. A* **1971**, *324*, 301−313.

(17) Gautam, K. S.; Dhinojwala, A. *Macromolecules* **2001**, *34*, 1137−1139.

(18) Shen, Y. R. *The Principles of Nonlinear Optics;* John Wiley & Sons, Inc.: New York, 1984.

(19) Bain, C. D. *Faraday Trans.* **1995**, *91*, 1281−1296.

(20) Harp, G. P.; Gautam, K. S.; Dhinojwala, A. *J. Am. Chem. Soc.* **2002**, *124*, 7908−7909.

(21) Harp, G. P.; Rangwalla, H.; Yeganeh, M. S.; Dhinojwala, A. *J. Am. Chem. Soc.* **2003**, *125*, 11283−11290.

(22) Qi, J.; Dillard, D. A.; Plaut, R. H.; Dillard, J. G. *J. Adhes.* **2003**, *79*, 559−579.

(23) Chaudhury, M. K.; Whitesides, G. M. *Langmuir* **1991**, *7*, 1013−1025.

(24) Barquins, M. *Mat. Sci. Eng.* **1985**, *73*, 45−63.

(25) Grosch, K. A. *Proc. R. Soc. London, Ser. A.* **1963**, *274*, 21−39.

(26) Homola, A. N.; Israelachvili, J. N.; Gee, M. L.; McGuiggan, P. M. *J. Tribol.* **1989**, *111*, 675−682.

(27) Newby, B. Z.; Chaudhury, M. K. *Langmuir* **1998**, *14*, 4865−4872.

(28) Socoliuc, A.; Bennewitz, R.; Gnecco, E.; Meyer, E. *Phys. Rev. Lett.* **2004**, *92*, 1343011−1343014.

(29) The absolute values of the shear stress reported in Figure 2 are different from those reported by Vorvolakos and Chaudhury.[12] One of the reasons for these differences could be due to different crosslink density of the PDMS lenses.

(30) Wu, S. *Polymer Interfaces and Adhesion;* Marcel Dekker: New York, 1982; Volume 1.

(31) The equations for the analysis of phenyl groups are discussed in Harp et al.[21] There is a error in eqs 11 and 12 in Harp et al.[21] and the right hand side of these two equations should be interchanged. The ratio of the Fresnel factors for SSP/SPS polarization at the incidence angle of 12° is ≈ 1 and we have used the ratio of $\beta_{aac}/\beta_{ccc} = 0.28$.

(32) Sills, S.; Overney, R. M. *Phys. Rev. Lett.* **2003**, *91*, 095501/1−09550.1/4.

(33) Schwab, A. D.; Dhinojwala, A. *Phys. Rev. E: Stat. Phys., Plasmas, Fluids, Relat. Interdiscip. Top.* **2003**, *67*, 0218021−0218029.